PCCP

Accepted Manuscript

ROYAL SOCIETY OF CHEMISTRY

www.rsc.org/pccp

PCCP

RSCPublishing

PAPER

Assessment of Density-Functionals for Describing the $X^- + CH_3ONO_2$ Gas-Phase Reactions with X = F, OH, CH_2CN†

Cite this: DOI: 10.1039/xoxxoooooox

Yaicel G. Proenza,[a] Miguel A. F. de Souza,[ab] Elizete Ventura,[b] Silmar A. do Monte[b] and Ricardo L. Longo*[a]

The energetic of the $E_{CO}2$, $S_N2@C$ and $S_N2@N$ channels of $X^- + CH_3ONO_2$ (X = F, OH, CH_2CN) gas-phase reactions were computed using the CCSD(T)/CBS method. This benchmark extends a previous study with X = OH [M. A. F. de Souza *et al*., *J. Am. Chem. Soc.* **2012**, *134*, 19004] and was used to ascertain the accuracy and robustness of nineteen density-functionals for describing these potential energy profiles (PEP) as well as the kinetic product distributions obtained from RRKM calculations. Assessments were based on the mean unsigned error (MUE), the mean signed error (MSE), the #best:#worst (BW) criterion and the statistical confidence interval (CI) for the MSE. In general, double-hybrids (DH) functionals perform better than the range-separated ones, and both are better than the global-hybrid functionals. Based on the MUE and CI criteria the B2GPPLYP, B2PLYP, M08-SO, BMK, ωB97X-D, CAM-B3LYP, M06, M08-HX, ωB97X and B97-K functionals show the best performance in the description of these PEPs. Within this set, the B2GPPLYP functional is the most accurate and robust. The RRKM results indicate that the DHs are the best for describing the selectivities of these reactions. Compared to CCSD(T), the B2PLYP method has a relative error of only *ca*. 1% for the selectivity and the accuracy to provide the correct conclusion concerning the nonstatistical behavior of these reactions.

Received ooth January 2014,
Accepted ooth January 2014

DOI: 10.1039/xoxxoooooox

www.rsc.org/

1. Introduction

Calculations of relative energies of physical and chemical processes with accuracy of 1.0 kcal mol^{-1} is one of the main challenges for computational chemistry.[1] Approximations to the density-functional theory (DFT) based Kohn-Sham formalism, termed generally as DFA (density-functional approximation),[2] are very popular due to a good compromise between computational effort and accuracy.[3] Indeed, DFAs have become very accurate, however, still have not reached this desired reliability. Most of these improvements are due to a deeper understanding of the role played by the exchange-correlation functional.[2-5]

Numerous attempts have been designed to take into account exchange effects, electron correlation and kinetic energy corrections to formulations of the exchange-correlation functional.[5-12] Therefore, benchmark calculations are a crucial tool to assess the reliability of these functionals.[12-20] Although benchmark sets have contributed significantly to the construction of functionals with increasing applicability and with minimum loss of accuracy, a fundamental outcome from several benchmark studies found in the literature is that most of the functionals are appropriate for particular sets of problems and systems.[17-20]

An accurate description of reaction channels is important to predict chemical selectivity using, for instance, the Rice-Ramsperger-Kassel-Marcus (RRKM) and transition state (TS) theories. Indeed, such accuracy may be used to test the limitations of these statistical theories for describing chemical selectivity.

In recent years a new paradigm is emerging in the theoretical-computational chemical kinetics,[21-23] when an experimental result does not agree with a prediction based on calculated barriers combined with statistical approach, it would usually be assumed that the calculated barriers are simply inaccurate and, rarely, that the statistical approach should not be applied to those reactions.[22,23] Frequently, such interpretation is the correct one, but the outcomes of several studies have suggested that this may not be the case, and the discrepancy may be due to the statistical theories.[24-26] Such change of interpretation can be attributed to: (i) the current possibility of computing potential energy profiles (PEPs) of reactions with highly accurate electronic structure methods, such as CCSD(T), MR-CISD, etc.; (ii) several limitations of the statistical approaches have been identified through comparisons between experimental results and the ones obtained from direct dynamics simulations of quasi-classical (and also classical) trajectories.[27]

Recently our group has shown that the products distribution of the $OH^- + CH_3ONO_2$ reaction is not properly described by the RRKM theory.[28,29] In this case, quasiclassical dynamics simulations have yielded a branching ratio in close agreement with experiment. These results suggest that the failure of the statistical approach can be a consequence of the following factors: (i) the long-range role of the electrostatic potential generated by the oxygen atoms in the ONO_2 moiety; (ii) occurrence of an apparently non-equilibrated reactant complex; and (iii) an excessive number of barrier recrossings.

The goal of the present work is to carry out a benchmark study using DFT methods for describing the $X^- + CH_3ONO_2$ (X = F, OH, CH_2CN) gas-phase reactions. These reactions can proceed via bimolecular nucleophilic substitution either at the carbon (S_N2@C) or the nitrogen center (S_N2@N) as well as a channel characterized by a proton abstraction followed by dissociation ($E_{CO}2$).[28] In addition, the products distribution strongly depends on the nucleophile (see Scheme 1), and there are evidences that their selectivities are not properly described by the RRKM theory,[29] which can be considered one of the most relevant characteristics of these systems. The reaction with OH^- nucleophile was previously studied with the CCSD(T)/CBS//MP2/6-311+G(3df,3p) method and two DFT functionals were tested for dynamics simulations.[29]

A key feature of the present investigation is to assess the accuracy of the selected density-functionals for kinetics applications. Thus, in addition to the relative barrier heights between the reaction pathways in Scheme 1, the product distributions obtained from the RRKM theory will also be used as comparative parameters. Therefore, an important issue is to determine which density-functional(s) is(are) able to indicate the inability of the statistical approach to describe the selectivity of the reactions in Scheme 1.

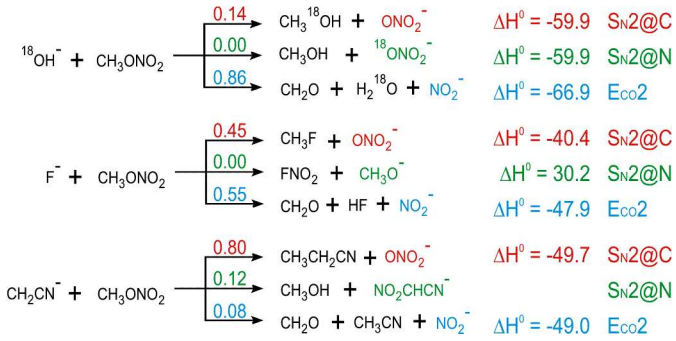

Scheme 1 Reaction channels for the $X^- + CH_3ONO_2$ (X = F, ^{18}OH, CH_2CN) systems with their experimental relative product distributions[28,30] and experimental ΔH^0 values[31] (in kcal mol^{-1}).

Several benchmark and assessment studies have been performed for multichannel gas-phase ion-molecule reactions in which base-induced eliminations compete with bimolecular nucleophilic substitutions.[32-34] However, the reactions presented in Scheme 1 have an additional S_N2 pathway (S_N2@C and S_N2@N) that imposes a more stringent test to the electronic structure and kinetics methods. In addition, the selectivity is highly dependent upon the nucleophile and all reaction channels are experimentally characterized.

In the present manuscript a total of nineteen DFT methods selected from those recommended in these latter studies have been used, and their performance will be tested through comparisons with CCSD(T)/CBS results. Traditionally, such type of comparison is focused on the mean unsigned error (MUE) and the mean signed error (MSE), which only takes into account the accuracy. However, a recent benchmark study suggests the use of the MSE/MUE pair with the BW criterion for a better assessment of a given functional.[1] The BW parameter is obtained by counting how often a given functional provides the best or the worst result.[1] Such a combination of criteria takes into account accuracy as well as robustness.

The present study deals with reactions containing channels whose barrier heights are in a reasonably large range (from 0.1 to 13.4 kcal mol^{-1}, at the CCSD(T)/CBS level). It is also worth to mention that differences between barrier heights of reaction channels are important to a proper description of the selectivity, and some of these differences are very small (less than 1 kcal mol^{-1}). Thus, a relative statistical parameter, the mean relative error (MRE), has been employed to treat all reaction channels on equal footing. Besides, we have suggested complementing the analysis of errors by a confidence interval, CI, obtained from a paired *Studentt*-test. Such criterion is meant to take into account the robustness of the functionals, as in the present case it encloses important numerical details not enclosed by BW. Therefore, in the present work the performance of the chosen functionals is based on the following set of statistical criteria: MSE, MUE, BW and CI.

2. Computational details

2.1. Electronic structure calculations

The reaction pathways shown in Scheme 1, involving the F^-, OH^-, CH_2CN^- + CH_3ONO_2 reactions have been investigated. All calculations were performed with the Gaussian 09,[35] GAMESS,[36,37] and ACES-III[38] programs. The stationary points along each reaction pathway were characterized with the MP2/6-311+G(3df,2p) method.[39-41] Intrinsic reaction coordinate (IRC) calculations were performed to ensure the correct connection between the transition state and their adjacent minima (reactant or product complexes). The nature of the stationary points was determined from the eigenvalues of the Hessian matrix, which were also used to compute the vibrational zero-point energies (ZPE). These calculations were performed with Gaussian 09 using its default criteria.

The benchmark consists of single-point energy calculations with the CCSD(T)[42] and DFT methods at the stationary points of each reaction channel. The CCSD(T) calculations were performed with the ACES-III program using the aug-cc-pVXZ (X = D, T, Q) basis sets,[43,44] which were extrapolated to the complete basis set (CBS) limit[45] using a two-point model with the optimized parameters of Truhlar[46] and Huh and Lee.[47] The DFT calculations were performed with the aug-cc-pVTZ basis sets using the GAMESS program, except for the mPW1K, BB1K and mPW1B95 functionals that were performed with the Gaussian 09 program.

The tested density-functionals are presented in Table 1. They comprise fourteen global hybrid (GH) functionals, three range-separated hybrid functionals (RS) and two double-hybrid functionals (DH). The first set includes two approaches: the generalized gradient approximation (GGA) and meta-GGA, which are distinguished by their independence or dependence on the kinetic energy density, hereafter denoted as HG and HM, respectively.

Table 1 Complete list of the nineteen density-functionals tested.

Method	Year	Type	Refs	Method	Year	Type	Refs
B3LYP	1994	HG	7,48	M05-2X	2006	HM	53
PBE0	1999	HG	49	B2PLYP	2006	DH	54
mPW1K	2000	HG	50	M06	2008	HM	55
B97-K	2004	HG	8	M06-2X	2008	HM	55
BMK	2004	HM	8	M08-HX	2008	HM	17
BB1K	2004	HM	10	M08-SO	2008	HM	17
mPW1B95	2004	HM	11	ωB97X	2008	RS	56
CAM-B3LYP	2004	RS	51	ωB97X-D	2008	RS	57
B97-3	2005	HG	52	B2GPPLYP	2008	DH	58
M05	2005	HM	9				

To ensure the reliability of our benchmark, the energy profiles of the F^- + CH_3ONO_2 and OH^- + CH_3ONO_2 reactions were investigated at higher computational levels, namely, *i*) the CCSD(T) energies were extrapolated to the CBS limit using the aug-cc-pVXZ basis sets with X = D, T and X = T, Q; and *ii*) the four best ranked functionals in the benchmark were employed in additional calculations with the larger aug-cc-pVQZ basis sets.

For the MP2, DHDFs, and CCSD(T) calculations, the core orbitals were excluded from the correlated treatment. Convergence tolerances of 10^{-6} and 10^{-4} hartree bohr^{-1} were used for the self-consistent field density and the gradient, respectively. Default Lebedev (96, 302) integration grid was used, except for the M06-2X, M08-HX and M08-SO functionals, which required a finer Lebedev (96, 590) grid. Noteworthy, convergence criteria tighter than 10^{-6} for the density and 10^{-4} hartree bohr^{-1} for the gradient as well as the necessity of a finer integration grid for the referred functionals have negligible effects on the computed energies.[19]

2.2. RRKM calculations

The rate constant for each reaction pathway in Scheme 1 was calculated with the quantum harmonic RRKM theory.[21,59] The microcanonical rate constant $k(E_i,J)$ depends on the internal energy (E_i) and angular momentum (J) of the reactants (R) through the equation:

$$k(E_i,J) = L^* \frac{W(E_i - E^*,J)}{hN(E_i,J)}$$

where h is the *Planck* constant, L^* is the degeneracy associated with each reaction channel symmetry, $W(E_i - E^*,J)$ is the number of roto-vibrational states of the TS with energies larger than the barrier height (E^*) and $N(E_i,J)$ is the density of roto-vibrational states. The $k(E_i,J)$ was computed with the Beyer-Swinehart algorithm[60] to determine the number of states implemented in the *SuperRRKM* program.[61]

The available internal energy was calculated as $E_i = \Delta E_{RC} + E_R - E_{RC}$, where ΔE_{RC} is the energy released upon formation of the most stable reactant complex (RC), E_R is the thermal contribution to the translational, rotational and vibrational energy of the separated reactants, and E_{RC} is the thermal contribution to the translational and rotational energy of the most stable RC. These thermal contributions were calculated at 298 K and rotational effects were not considered ($J = 0$). This procedure to compute E_i has been successfully applied to estimate the product distributions of several gas-phase reactions.[62-66] The calculated values of E^* as well as the geometries, energies and vibrational frequencies are available in the Electronic Supplementary Information (ESI).

2.3. Assessment of the density-functionals

The performance of the DFT/aug-cc-pVTZ//MP2/6-311+G(3df,2p) methods was assessed by comparing the energies and the product distributions (obtained from the RRKM calculations) with those from the reference CCSD(T)/CBS(D,T)//MP2/6-311+G(3df,2p) method, for each reaction in Scheme 1. This assessment was based on the MUE/MSE and BW descriptors, along with the two complementary criteria MRE and the paired *Student t*-test CI expressed as,

$$\mathrm{MUE} = \frac{1}{n}\sum_{i=1}^{n}|d_i| \qquad \mathrm{MSE} = \frac{1}{n}\sum_{i=1}^{n} d_i \qquad \mathrm{MRE}(\%) = \frac{100}{n}\sum_{i=1}^{n}\frac{d_i}{y_i}$$

$$S_d = \sqrt{\frac{\sum_{i=1}^{n}(d_i - \mathrm{MSE})^2}{n-1}} \qquad \mathrm{CI} = \mathrm{MSE} \pm t_{\alpha/2}\frac{S_d}{\sqrt{n}}$$

where $d_i = y_i - x_i$, and the values y_i and x_i are the energies of the *i*-th stationary point (relative to separated reactants, Rs) computed with the CCSD(T) and DFT methods, respectively. S_d is the standard deviation of the differences, $t_{\alpha/2}$ is the critical *t*-value for two-tails with n – 1 degrees of freedom, and α = 0.01 is the statistical significance of the CI.[67]

The BW criterion is obtained as follows: *i*) the unsigned error is computed for each stationary point and then it is checked which functional yields the best and the worst result; *ii*) each time a given functional yields the best result, 1 is incremented into the #best descriptor and the same holds for the #worst descriptor when a functional yields the worst result.

3. Results and discussion

3.1. Potential energy profiles of the reaction pathways

A more detailed description of the PEP of the F^-, OH^-, CH_2CN^- + CH_3ONO_2 reactions, calculated at the CCSD(T)/CBS(D,T)//MP2/6-311+G(3df,2p) level, is shown in Fig. 1. Notice that all PEPs display the typical profile of the *double-well* model for ion-neutral gas-phase reactions, supported both experimentally and theoretically.[68-70] Moreover, like for most exothermic gas-phase ion-molecule reactions, the ion-dipole complexes (RCs and PCs) and the transition states (TSs) are lower in energy than the corresponding separated reactants. Such feature support the observed reaction efficiencies for these type of reactions.[28,30] Another characteristic of these reactions is the high exothermicity of the channels, which are consistent with the experimental reaction enthalpies (see Scheme 1).

Noteworthy that the energies of the stationary points of the F^-+ CH_3ONO_2 and OH^- + CH_3ONO_2 reactions were also extrapolated to the CBS limit using the aug-cc-pVXZ (X = T, Q) basis sets. The results (Table S9 in ESI) are near identical to those obtained through the (X = D, T) extrapolation, with differences smaller than 1 kcal mol^{-1}. This corroborates the reliability and the accuracy of the CCSD(T)/CBS(D,T) results and its use for the larger system.

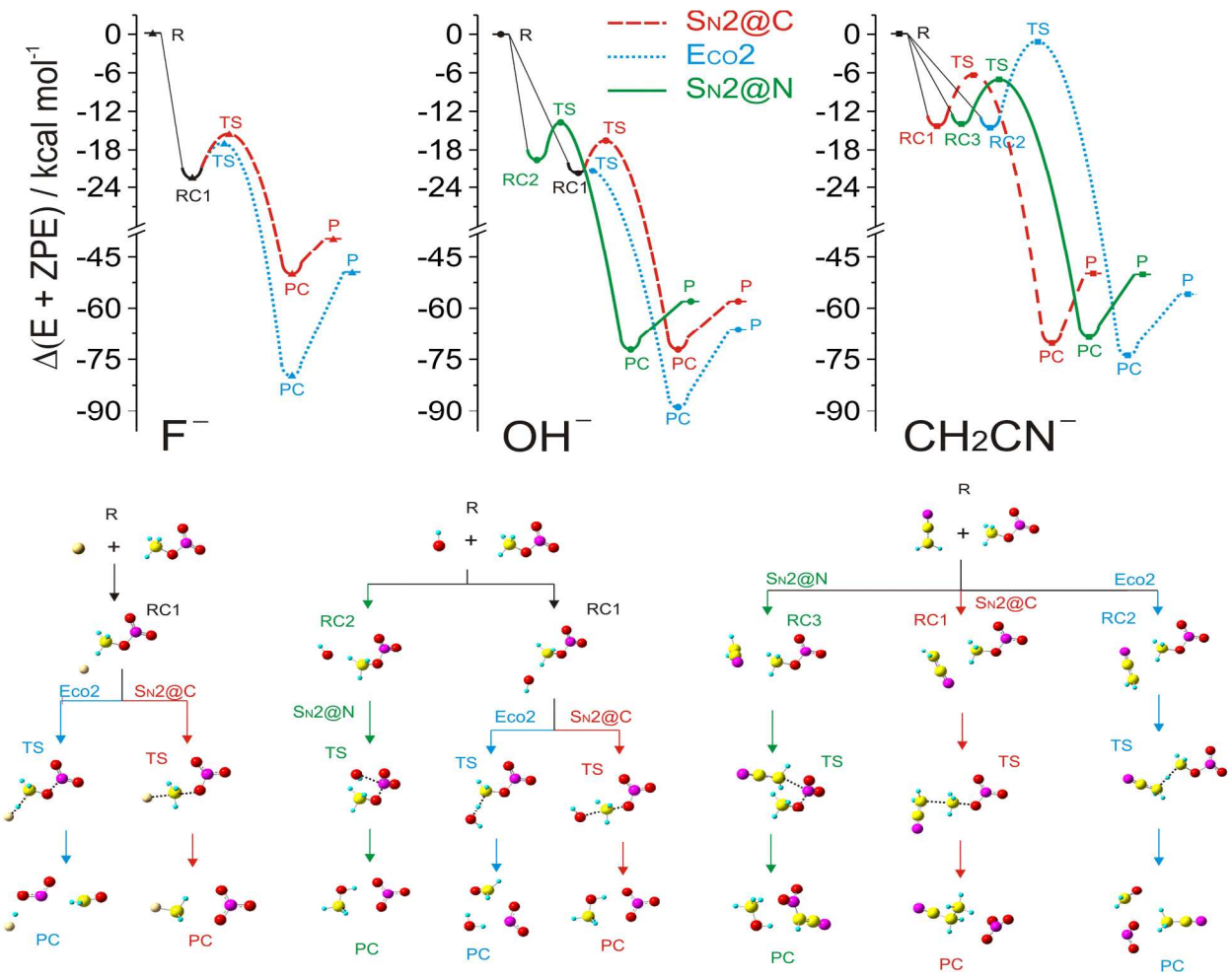

Fig. 1 *Top panel*: PEP of the F^-, OH^-, CH_2CN^- + CH_3ONO_2 reactions, calculated at the CCSD(T)/CBS//MP2/6-311+G(3df,2p) level. The results of the OH^- + CH_3ONO_2 reaction were adapted from Figure 1 in ref. 29. The energies (in kcal mol^{-1}) are relative to the separated reactants and include ZPE corrections. *Lower panel*: the structures of the relevant stationary points are depicted (Cartesian coordinates can be found in the ESI). *Notation*: reactants (R), reactant complex (RC), transition state (TS), product complex (PC) and products (P).

F^- + CH_3ONO_2 system. According to our calculations, the S_N2@C and $E_{CO}2$ pathways start at the reactant complex RC1 with energy of -23.8 kcal mol^{-1}. The S_N2@C channel then proceeds through a TS at -16.8 kcal mol^{-1} and yields the CH_3F and NO_3^- products. The $E_{CO}2$ channel involves a TS at -18.3 kcal mol^{-1} ends up in the very exothermic HF, CH_2O and NO_2^- products (see Figure 1). For the F^- nucleophile the results suggest that the $E_{CO}2$ pathway is slightly preferred over the S_N2@C (the relative difference between the calculated barrier heights is 1.5 kcal mol^{-1}), which agrees qualitatively with the experimental selectivity (see Scheme 1). For the S_N2@N pathway, the experimental ΔH^0 suggests that the anionic product is not likely to be formed, as this channel is highly endothermic and, indeed, no methoxide ion has been detected experimentally.[28] Therefore, this reaction pathway was not considered in the assessment.

OH^- + CH_3ONO_2 system. The calculations show a richer PEP[29] than the one obtained for the F^- nucleophile because in addition to the reactant complex RC1 associated with both S_N2@C and $E_{CO}2$ pathways, a different reactant complex RC2 (with the nucleophile bonded to the proton off the symmetry plane, see Fig. 1) was found for the S_N2@N pathway. Their energies are -21.7 and -19.6 kcal mol^{-1}, respectively. The $E_{CO}2$ channel involves a TS of -21.7 kcal mol^{-1}, while the S_N2@C and S_N2@N pathways proceed through TSs with energies of -16.5 and -14.2 kcal mol^{-1}, respectively. In the case of OH^-, our calculations suggest that the $E_{CO}2$ pathway is highly preferred over the S_N2 and consists of a virtually barrier less process (see Fig. 1). These results agree qualitatively with the experimental product distributions (see Scheme 1). Finally, these three pathways lead to thermodynamically more stable products than the ones obtained with F^-.

CH_2CN^- + CH_3ONO_2 system. Experimentally, Moran and co-workers[71] have shown that the cyanomethyl anion with the negative charge localized on the methylenic C atom reacts much faster than the resonance hybrid with a negative charge on N. Therefore, we have considered only the reaction through the terminal carbon atom of the nucleophile. As observed in Fig. 1, the calculated PEPs differs

significantly from the previous reactions, namely, a different RC was found for each channel. Another important difference is the lower stabilities of the RCs, with energies of -14.4, -14.7 and -14.0 kcal mol^{-1} for RC1, RC2 and RC3, respectively. The S_N2@C pathway involves RC1 that goes through a TS of -6.6 kcal mol^{-1} and ends up in the CH_3CH_2CN and NO_3^- products, again associated with a high exothermicity. Analogously, the S_N2@N channel starts at RC3 that is connected to a TS of-7.2 kcal mol^{-1} and leads to the final CH_3OH and $NCCHNO_2^-$ products. The $E_{CO}2$ channel is unlikely to reach the TS of -1.3 kcal mol^{-1} due to its large barrier (see Fig. 1), which significantly disfavors the $E_{CO}2$ pathway compared to both nucleophilic displacements.

3.2. Assessments of density-functionals for describing the potential energy profiles

Table 2 shows two types of MUE values obtained for all tested functional. One, denoted as Overall, is calculated from the whole set of stationary points of the three systems, while the other takes into account each reaction separately for which the MRE values were included. The MSE parameter was also calculated from the whole set of stationary points and the CI for the MSE is presented.

For the $OH^- + CH_3ONO_2$ reaction, the mPW1K, PBE0 and M06-2X functionals show MUE values larger than 2.5 kcal mol^{-1}, while four (B2GPPLYP, B2PLYP, B3LYP and CAM-B3LYP) have MUE values lower than 1.0 kcal mol^{-1}. When the nucleophile is CH_2CN^- and employing the same threshold values, the corresponding worst functionals are M05, BB1K, mPW1K and PBE0, whereas the best set includes B2GPPLYP and M08-SO. In the case of the $F^- + CH_3ONO_2$ reaction, only the mPW1K functional has a MUE value larger than 2.5 kcal mol^{-1}, while none of the tested functionals has a MUE value smaller than 1.0 kcal mol^{-1}, but the B2GPPLYP functional has MUE (1.03 kcal mol^{-1}) very close to this threshold. The best accuracy was provided by the B2GPPLYP functional in the $OH^- + CH_3ONO_2$ reaction (MUE = 0.56 kcal mol^{-1}), while the worst was obtained with the M05 functional in the $CH_2CN^- + CH_3ONO_2$ reaction (MUE = 3.04 kcal mol^{-1}). Only the mPW1K functional is simultaneously in the worst set of the three reactions, while only the B2GPPLYP functional can be regarded as being in the best sets of all pathways of these three reactions.

It is noteworthy that the largest MRE values were obtained for the $CH_2CN^- + CH_3ONO_2$ reaction. This is due to the smaller energies of the TSs relative to the Rs compared to those of the other reactions (see Fig. 1). For instance, the MUE of BMK for the $OH^- + CH_3ONO_2$ reaction is 1.72 kcal mol^{-1} that corresponds to a MRE of 3.0%. On the other hand, for the $CH_2CN^- + CH_3ONO_2$ reaction, a smaller MUE of 1.64 kcal mol^{-1} was obtained with the CAM-B3LYP functional that corresponds to a higher MRE of 10.5%.

In order to find which density-functionals show the best and worst accuracy for the whole set of reactions the overall MUE needs to be taken into account. Considering that (i) MUE values smaller than 2-3 kcal mol^{-1} were usually taken as a reasonable threshold for DFT methods[16,32-34] (ii) the tested functionals show good accuracy in gas-phase ion-molecule reactions[1,2,17,32-34,72,73] and (iii) in the present study these functionals are intended to be applied in kinetics studies, a value of 2 kcal mol^{-1} shall be considered as the cutoff criterion to classify the functionals.

Table 2 MUE (kcal mol^{-1}) and MRE (%, in parentheses) of density-functionals for the potential energy profiles (PEPs) of the F^-, OH^-, $CH_2CN^- + CH_3ONO_2$ reactions. The CI (in kcal mol^{-1}) for the MSE considering all the PEPs is also included.

Method [a]	OH^-	CH_2CN^-	F^-	Overall [b]	CI [c]
B2GPPLYP	0.56 (1.52)	0.70 (3.99)	1.03 (2.82)	0.76	(-0.97; -0.16)
B2PLYP	0.78 (2.02)	1.10 (4.80)	1.35 (3.41)	1.08	(-1.41; -0.29)
M08-SO	1.94 (5.73)	0.72 (6.10)	1.28 (4.15)	1.31	(+0.15; +1.57)
CAM-B3LYP	0.98 (2.24)	1.64 (10.49)	1.31 (3.82)	1.31	(-1.57; +0.06)
ωB97X-D	1.17 (2.92)	1.28 (8.02)	1.84 (5.41)	1.43	(-1.88; -0.15)
BMK	1.72 (3.00)	1.29 (8.43)	1.46 (4.67)	1.49	(-0.25; +1.82)
M06	1.21 (4.36)	2.12 (9.82)	1.42 (3.71)	1.58	(-1.93; +0.23)
B3LYP	0.88 (1.98)	2.29 (10.37)	1.59 (4.75)	1.59	(-2.18; -0.22)
B97-K	1.59 (3.91)	1.41 (11.95)	1.81 (6.18)	1.60	(-0.98; +1.13)
ωB97X	1.31 (2.84)	1.42 (10.02)	2.24 (7.43)	1.66	(-1.83; +0.27)
M08-HX	2.49 (7.72)	1.30 (8.47)	1.48 (4.08)	1.76	(+0.04; +1.96)
mPW1B95	1.40 (2.82)	2.33 (8.43)	1.63 (3.46)	1.79	(-2.51; +0.01)
B97-3	1.61 (5.15)	2.38 (12.47)	1.84 (5.16)	1.94	(-2.51; -0.34)
M06-2X	2.62 (8.50)	1.29 (7.21)	1.96 (5.63)	1.96	(+0.37; +2.43)
M05-2X	2.27 (7.62)	1.81 (15.63)	2.46 (7.67)	2.18	(-0.20; +2.29)
M05	1.53 (4.27)	3.04 (16.94)	2.24 (6.42)	2.27	(-3.32; -1.12)
BB1K	1.80 (4.43)	2.66 (22.20)	2.47 (8.25)	2.31	(-2.64; +0.18)
mPW1K	2.53 (5.84)	2.72 (14.55)	2.56 (7.63)	2.60	(-2.57; +0.98)
PBE0	2.53 (6.48)	3.02 (16.81)	2.41 (6.89)	2.65	(-3.37; +0.50)

[a] All absolute DFT/aug-cc-pVTZ energies are given in the ESI. The ZPE correction is not included. [b] The values are listed in ascending order. [c] Calculated with the paired *t*-test using $n = 28$ and $\alpha = 0.01$.

The best results were obtained with the B2GPPLYP, B2PLYP, M08-SO, CAM-B3LYP, ωB97X-D and BMK functionals, with overall MUE values smaller than 1.50 kcal mol^{-1}, where the B2GPPLYP functional shows the best result (MUE = 0.76 kcal mol^{-1}) towards the desired accuracy of electronic structure calculations. The overall MUE values of the last five entries in Table 2 (M05-2X, M05, BB1K, mPW1K and PBE0) are larger than the cutoff value of 2 kcal mol^{-1}, even though the mPW1K and BB1K functionals being designed for kinetics studies.[10,50] However, even the largest overall MUE value (2.65 kcal mol^{-1} for PBE0) may be regarded as a good result, because it falls within the 2-3 kcal mol^{-1} range employed to gauge the reliability of DFT approximations.

The assessments of all density-functionals shall be ascertained through a joint analysis of their accuracy and robustness. As aforementioned a suggested parameter associated with the robustness of functionals is BW. The calculated BW values are shown in Fig. 2. The results are in line with the improvement of the DFA's in the last few decades, suggesting that the DH are more adequate than the RS methods, and both perform much better than the HG and HM functionals, see Fig. 2(b).

From Fig. 2 it is clear that the B3LYP, M06, M08-HX, M05, mPW1K, PBE0, M05-2X and BB1K functionals show more worst than best results. Therefore, the BW criterion suggests that such functionals are not robust. It is important to mention that this set contains the five functionals (M05, mPW1K, PBE0, M05-2X and BB1K) with overall MUE values larger than the cutoff (compare Fig. 2 and Table 2).

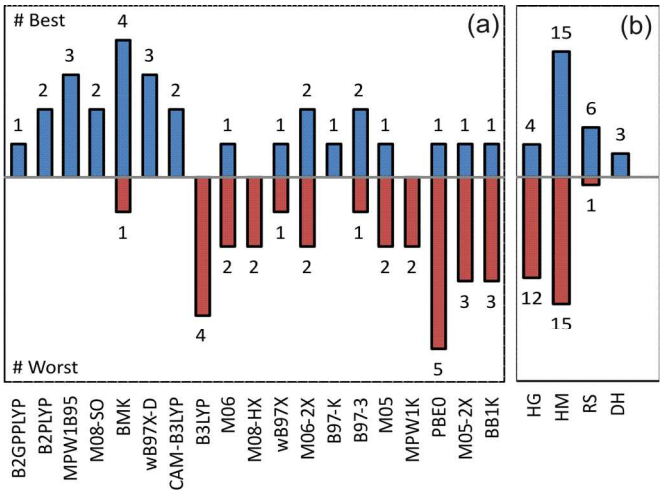

Fig. 2 BW values obtained from the unsigned errors (see text for details) for (a) all tested functionals and (b) functionals that share the same theoretical approach.

The BW of the ωB97X-D and mPW1B95 functionals (#best:#worst, 3:0) may suggest that they are more robust than B2GPPLYP (1:0). However, these outcomes are not in line with the analysis of the corresponding overall MUE, as these values for ωB97X-D and mPW1B95 are 88% and 135% larger than that of the B2GPPLYP, respectively. Moreover, the B2GPPLYP functional shows the best accuracy for all three reactions (see Table 2). Thus, in the present study the BW seems to work only as a rough criterion, which should not be interpreted without the MUE parameter.

Therefore, it is suggested that using the CI for the MSE (see Table 2) should provide a more adequate evaluation of the robustness and would complement the overall MUE parameter. The CI limits (absolute values) are chosen to be 2 kcal mol^{-1} in order to be consistent with the cutoff of 2 kcal mol^{-1} employed for the overall MUE. Notice that the functionals with lower accuracy (M05-2X, M05, BB1K, mPW1K and PBE0), according to the overall MUE, also have CI limits outside this cutoff. However, four functionals (M06-2X, B3LYP, mPW1B95 and B97-3) with overall MUE values lower than 2 kcal mol^{-1} lack robustness because they have one of the CI limits larger than the threshold value (see Table 2). Thus, the following ten density-functionals: B2GPPLYP, B2PLYP, M08-SO, CAM-B3LYP, ωB97X-D, BMK, M06, B97-K, ωB97X and M08-HX may be considered as having good performance because they are simultaneously accurate and robust (see Table 2).

It is noteworthy that the results in ref. 29 for the M06-2X functional are better than the ones presented in Table 1 for the OH^- + CH_3ONO_2 reaction because in this previous study, the critical points in the PEP were obtained at the M06-2X level,[29] whereas the assessments presented here are performed considering the critical points determined with the MP2 method.

In order to align the CI criterion with the goals of the present benchmark study we take into account the following additional features: the CI size, the proximity of the CI limits to zero, and the signs of CI limits. As a result, B2GPPLYP has the best CI, as its size is the smallest, at least one of its limits is very close to zero and both limits have the same sign. The CI for this functional varies between -0.97 and -0.16 kcal mol^{-1}, which means that this is the only functional that predicts 99% of the deviations within 1 kcal mol^{-1} from the CCSD(T)/CBS results. This result is consistent with the outcome from the MUE analysis because this functional has the smallest overall MUE value (see Table 2).

Notice that the CI values for the B97-K and M06 functionals range from -0.98 to +1.13 and from -1.93 to +0.23 kcal mol^{-1}, respectively. These functionals also show good accuracy based on the overall MUE values. However, considering the additional features required to achieve full robustness of CI, their results are not adequate. Both functionals have similar undesirable large CI values (2.11 and 2.16 kcal mol^{-1}, respectively) and their CI limits reveal that the errors distribution is not uniform, which means that they can either overestimate or underestimate the energies of the stationary points with the same probability. Conversely, in the case of the M06 functional the magnitude of its most positive error is very small (0.23 kcal mol^{-1}).

Additional calculations for the F^- and OH^- + CH_3ONO_2 systems were performed with the best-ranked functionals (B2GPPLYP, B2PLYP, M08-SO and CAM-B3LYP) using the larger aug-cc-pVQZ basis sets. These calculations intended to evaluate possible basis sets dependence of the functionals performance (Table S10 and S11 in ESI). Indeed, the energy differences between the X = Q and X = T basis sets results were smaller than 0.4 kcal mol^{-1} for all stationary points of all reaction channels. Thus, the results obtained with the aug-cc-pVTZ basis sets seem to have the appropriate accuracy and convergence.

3.3. Accuracy of density-functionals for relative barrier heights and $E_{CO}2$:S_N2@C:S_N2@N relative distribution

The successful description of barrier heights (E*) for the reaction pathways and of their relative differences (ΔE*) is fundamental for providing appropriate selectivity and kinetics. In our case, the ΔE* values of some reaction channels can be very small (smaller than 1 kcal mol^{-1} at the CCSD(T)/CBS level), as for example, the ΔE* between the S_N2@C and S_N2@N channels of the CH_2CN^- + CH_3ONO_2 reaction is 0.6 kcal mol^{-1}, while for the F^- + CH_3ONO_2 reaction, the ΔE* between the S_N2@C and $E_{CO}2$ channels is 1.5 kcal mol^{-1} (see Fig. 1). Therefore, even though the ten functionals listed above have shown good to excellent accuracy for describing the PEPs, it is crucial to analyze their reliability concerning E* and ΔE*.

Table 3 Relative barrier heights (in kcal mol^{-1}) between channels obtained with relevant methods. All differences are relative to the $E_{CO}2$ channel.

Method	OH^-		CH_2CN^-		F^-
	C – E	N – E	C – E	N – E	C – E
CCSD(T)	+5.1	+7.4	-5.3	-5.9	+1.5
B2GPPLYP	+4.2 (-0.9)	+6.8 (-0.6)	-5.4 (-0.1)	-6.1 (-0.2)	+0.5 (-1.0)
B2PLYP	+4.0 (-1.1)	+6.6 (-0.8)	-5.2 (+0.1)	-5.7 (+0.2)	+1.7 (+0.2)
M08-SO	+6.0 (+0.9)	+7.2 (-0.2)	-5.3 (0.0)	-7.8 (-1.9)	-0.7 (-2.2)
CAM-B3LYP	+5.8 (+0.7)	+8.3 (+0.9)	-3.3 (+2.0)	-4.2 (+1.7)	-0.2 (-1.7)
ωB97X-D	+6.6 (+1.5)	+8.9 (+1.5)	-3.2 (+2.1)	-4.0 (+1.9)	+0.6 (-0.9)
BMK	+5.4 (+0.3)	+7.9 (+0.5)	-4.4 (+0.9)	-5.3 (+0.6)	-0.7 (-2.2)
M06	+6.6 (+1.5)	+5.9 (-1.5)	-3.4 (+1.9)	-7.4 (-1.5)	+3.0 (+1.5)
B97-K	+4.7 (-0.4)	+8.9 (+1.5)	-5.0 (+0.3)	-4.1 (+1.8)	-1.7 (-3.2)
ωB97X	+5.5 (+0.4)	+7.7 (+0.3)	-4.0 (+1.3)	-4.7 (+1.2)	-2.5 (-4.0)
M08-HX	+6.6 (+1.5)	+7.5 (+0.1)	-3.9 (+1.4)	-6.8 (-0.9)	+0.2 (-1.3)

C, N and E are used to identify the S_N2@C, S_N2@C and $E_{CO}2$ channels respectively. In parentheses are the deviations (in kcal mol^{-1}) with respect to the CCSD(T) results, $\Delta E^*_{DFT} - \Delta E^*_{CCSD(T)}$. The results for all tested functionals are shown in the ESI.

As the importance of barrier heights (E*) was already considered in the previous assessments of the functionals (section 3.3), Table 3 only presents the ΔE* values that were calculated taking the $E_{CO}2$ channel as the reference. These selected functionals show positive as well as negative errors (see Table 3) compared to the CCSD(T)/CBS results. Moreover, the functional considered as the best or worst depends on the reaction. For a given reaction, the best functionals for kinetics studies should have small errors relative to the reference method and such errors should have the same sign for all reaction channels. For the OH^- + CH_3ONO_2 reaction, the ωB97X and BMK functionals show the best accuracies and the former has errors of *ca*. 0.35 kcal mol^{-1} for both the S_N2@C and S_N2@N channels. In the case of the CH_2CN^- + CH_3ONO_2 reaction, the B2GPPLYP and B2PLYP functionals show equally the best accuracies, with errors of -0.1 and -0.2 kcal mol^{-1}, and of +0.1 and +0.2 kcal mol^{-1}, respectively. For the F^- + CH_3ONO_2 reaction, the B2PLYP, B2GPPLYP and ωB97X-D functionals are the most accurate, with B2PLYP having the smallest error (+0.2 kcal mol^{-1}).

The M08-SO, B97-K, M08-HX and M06 functionals show different signs between the channels compared to the CCSD(T)/CBS results (see Table 3). M06 shows the worst accuracy because it has relatively large errors and different signs between the channels that lead to an inversion of the S_N2@C:S_N2@N selectivity for the CH_2CN^- and OH^- + CH_3ONO_2 reactions compared to the CCSD(T)/CBS calculations. Notice that no other functional reverses the selectivity of these reactions. On the other hand, the ωB97X, BMK, ωB97X-D and CAM-B3LYP functionals present errors with the same signs, although they can be relatively large for some pathways compared to the other functionals. Therefore, the DH functionals B2PLYP and B2GPPLYP are the most accurate.

The RRKM results for the $E_{CO}2$:S_N2@C:S_N2@N branching ratios calculated with the CCSD(T)/CBS//MP2/6-311+G(3df,2p) reference method and with the ten density-functionals previously selected are shown in Table 4.

Table 4 Product distributions ($E_{CO}2$:S_N2@C:S_N2@N) for the F^-, OH^-, CH_2CN^- + CH_3ONO_2 reactions. The calculated values were obtained with the RRKM theory.

Method	$E_{CO}2$:S_N2@C:S_N2@N		
	F^-	OH^-	CH_2CN^-
Experimental[27,29]	55:45:0	86:14:0	8:80:12
CCSD(T)	83:17:0	99:1:0	0:59:41
B2GPPLYP	63:37:0	98:1:1	0:59:41
B2PLYP	84:16:0	98:1:1	0:60:40
M08-SO	60:40:0	[a]	0:18:82
CAM-B3LYP	67:33:0	[a]	0:53:47
ωB97X-D	76:24:0	[a]	0:46:54
BMK	60:40:0	[a]	0:46:54
M06	91:09:0	[a]	0:03:97
B97-K	46:54:0	99:1:0	0:90:10
ωB97X	34:66:0	99:1:0	0:49:51
M08-HX	71:29:0	[a]	0:10:90

[a] Not calculated due to negative values obtained for the barrier heights (E*) of the $E_{CO}2$ channel.

From the first two entries in Table 4, it is clear that the CCSD(T)/CBS results for the calculated product distributions are in disagreement with the experimental data.[28,30] However, for the OH^-+ CH_3ONO_2 reaction, the results obtained from quasi-classical trajectory simulations are in good agreement with the experimental results, which can be explained by the nonstatistical behavior of this system.[29] Is is thus very likely that the same behavior would be present for the other nucleophiles.

From the first two entries in Table 4, it is clear that the CCSD(T)/CBS results for the calculated product distributions are in disagreement with the experimental data.[28,30] However, for the OH^-+ CH_3ONO_2 reaction, the results obtained from quasi-classical trajectory simulations are in good agreement with the experimental results, which can be explained by the nonstatistical behavior of this

system.[29] Is is thus very likely that the same behavior would be present for the other nucleophiles.

All methods for which the branching ratios for the $OH^- + CH_3ONO_2$ reaction could be obtained indicated the near exclusive preference for the $E_{CO}2$ channel (see Fig. 1 and Table 3). Although relatively large errors in ΔE^* values were observed for this reaction (see Table 3), they are not enough to alter the calculated branching ratios. However, for the other two reactions the opposite behavior was found. For instance, the ΔE^* errors of the B97-K functional for the $OH^- + CH_3ONO_2$ reaction do not alter the branching ratios, however, similar ΔE^* errors for the $CH_2CN^- + CH_3ONO_2$ reaction significantly alter the $E_{CO}2$:S_N2@C:S_N2@N relative distribution.

The same holds for the ωB97X functional with respect to the OH^- and $F^- + CH_3ONO_2$ reactions. Thus, all density-functionals suggest a nonstatistical behavior for the $OH^- + CH_3ONO_2$ reaction in agreement with the CCSD(T) results.

In the assessment of the functionals for the branching ratios of the $CH_2CN^- + CH_3ONO_2$ reaction, the ΔE^* parameter between the S_N2@C and S_N2@N channels seems to be more important than between the S_N2 and $E_{CO}2$ pathways, because the S_N2 channels have very similar E^* values and the $E_{CO}2$ pathway is highly disfavored (see Fig. 1). For this reaction, the M0*x* functionals are the only ones that show a reverse selectivity between the S_N2@N and S_N2@C channels in comparison to the CCSD(T) results (see Table 4). These results are consistent with the trend shown by these functionals, namely, relatively large errors and different signs for the S_N2@C and S_N2@N channels (see Table 3).

Except the B97-K functional, all remaining DFA methods show good agreement with the CCSD(T) branching ratios (see Table 3). The $E_{CO}2$:S_N2@C:S_N2@N relative distribution obtained with the B97-K functional is closer to the experimental data than that calculated with CCSD(T) method. Thus, this is the only functional that could lead to an incorrect conclusion concerning the statistical behavior of this reaction.

For the $F^- + CH_3ONO_2$ reaction, Table 4 shows that the branching ratios obtained with following six functionals: B2GPPLYP, M08-SO, CAM-B3LYP, BMK, B97-K and ωB97X are in reasonable agreement with the experimental data. Thus, if one incorrectly assumes a statistical behavior for this reaction, the straightforward conclusion is that the small disagreements are due to errors in the calculated ΔE^* values. Therefore, one would follow an unadvised strategy of trying to improve these functionals in order to get a better description of the ΔE^* values. On the other hand, the remaining density-functionals predict the branching ratios in better agreement with the CCSD(T) values, especially the B2PLYP functional.

Conclusions

The assessments of the B3LYP, PBE0, mPW1K, B97-K, BMK, BB1K, mPW1B95, CAM-B3LYP, B97-3, M05, M05-2X, B2PLYP, M06, M06-2X, M08-HX, M08-SO, ωB97X, ωB97X-D and B2GPPLY density-functionals with respect to CCSD(T)/CBS reference method in describing the potential energy profiles, the relative barrier heights and the product distributions in the $E_{CO}2$, S_N2@N and S_N2@C channels of the F^-, OH^-, and $CH_2CN^- + CH_3ONO_2$ gas-phase reactions were performed. The mean unsigned error (MUE), the mean signed error (MSE), the BW criterion and the statistical confidence interval (CI) for the MSE parameters were used as statistical criteria for these assessments.

Based on a cutoff value of 2 kcal mol^{-1} for the overall MUE parameter, the M05, mPW1K, PBE0, M05-2X and BB1K functionals are not accurate enough for describing the PEPs of these reactions. The BW and CI parameters were used to check the robustness of the remaining functionals. As the former lacks consistency for these reactions, the CI for the MSE was used to evaluate the robustness of the density-functionals and to complement the overall MUE parameter. According to these criteria the functionals B2GPPLYP, B2PLYP, M08-SO, BMK, ωB97X-D, CAM-B3LYP, M06, M08-HX, ωB97X and B97-K show the best performance in the description of the PEPs. According with its CI, the B2GPPLYP is the only functional that predicts 99% of the deviations within 1 kcal mol^{-1} from the CCSD(T)/CBS reference results. The good performance of DH functionals was also observed in previous benchmark studies.[1,74,75]

These latter ten functionals were then used to compute the relative barrier heights and the $E_{CO}2$:S_N2@C:S_N2@N relative distribution for these three reactions. The two DH functionals B2GPPLYP and B2PLYP show the best results regarding these two properties relative to the CCSD(T)/CBS results. It is noteworthy the very good performance of the B2PLYP functional, with a relative error of *ca*. 1% for the selectivity. Therefore, this is the only functional that could lead to correct conclusions regarding the nonstatistical behavior of these reactions.

Acknowledgements

The Brazilian Agencies CNPq, CAPES, FACEPE, and FINEP are acknowledged for providing partial financial support under grants Pronex APQ-0859-1.06/08 and INCT-INAMI, and the regional computer centers CENAPAD-PE and CENAPAD-UFC for computational support. Y.G.P. thanks FACEPE for a graduate scholarship and MAFS thanks CNPq for fellowships.

Notes and references

[a] Departamento de Química Fundamental, CCEN, Universidade Federal de Pernambuco, Cidade Universitária, Recife, PE,50.740-560, Brazil.
[b] Departamento de Química, CCEN, Universidade Federal da Paraíba, João Pessoa, PB, 58.059-900, Brazil.
*E-mail: longo@ufpe.br; Fax: +55 81 21268442.

† Electronic Supplementary Information (ESI) available. See DOI: 10.1039/b000000x

1 L. Goerigk and S. Grimme, *Phys. Chem. Chem. Phys.*, 2011, **13**, 6670.
2 A. D. Becke, *J. Chem. Phys.*, 2014, **140**, 18A301.
3 A. J. Cohen, P. Mori-Sánchez and W. Yang, *Chem. Rev.*, 2012, **112**, 289.
4 M. L. Hall, J. Zhang, A. D. Bochevarov and R. A. Friesner, *J. Chem. Theory Comput.*, 2010, **6**, 3647.
5 L. Goerigk and S. Grimme, *J. Chem. Theory Comput.*, 2011, **7**, 291.

6 P. J. Stephens, F. J. Devlin, C. F. Chabalowski and M. J. Frisch, *J. Phys. Chem.*, 1994, **98**, 11623.
7 W. Kohn, A. D. Becke and R. G. Parr, *J. Phys. Chem.*, 1996, **100**, 12974.
8 A. D. Boese and J. M. L. Martin, *J. Chem. Phys.*, 2004, **121**, 3405.
9 Y. Zhao, N. E. Schultz and D. G. Truhlar, *J. Chem. Phys.*, 2005, **123**, 161103.
10 Y. Zhao, B. J. Lynch and D. G. Truhlar, *J. Phys. Chem. A*, 2004, **108**, 2715.
11 Y. Zhao and D. G. Truhlar, *J. Phys. Chem. A*, 2004, **108,** 6908.
12 M. J. G. Peach, T. Helgaker, P. Salek, W. K. Thomas, O. B. Lutnaes, J. T. David and N. C. Handy, *Phys. Chem. Chem. Phys.*,2006, **8**, 558.
13 S. Parthiban, G. De-Oliveira and J. M. L. Martin, *J. Phys. Chem. A*, 2001, **105**, 895.
14 T. Chen-Wei, S. Yu-Chuang, L. Guan-De and C. Jeng-Da, *Phys. Chem. Chem. Phys.*, **15**, 2013, 8352.
15 A. P. Bento, M. Solà and F. M. Bickelhaupt, *J. Comput. Chem.*, 2005, **26**, 1497.
16 Y. Zhao, N. G. García and D. G. Truhlar, *J. Phys. Chem. A*, 2005, **109**, 2012.
17 Y. Zhao and D. G. Truhlar, *J. Chem. Theory Comput.*, 2008, **4**, 1849.
18 O. Tishchenko and D. G. Truhlar, *J. Phys. Chem. Lett.*, 2012, **3**, 2834.
19 F. Yu, *J. Comput. Chem.*, 2012, **33**, 1347.
20 S. Zahn, D. R. MacFarlane and E. I. Izgorodina, *Phys. Chem. Chem. Phys.*, **15**, 2013, 13664.
21 U. Lourderaj and W. L. Hase, *J. Phys. Chem. A*, 2009, **113**, 2236.
22 B. K. Carpenter, *Annu. Rev. Phys. Chem.*, 2005, **56**, 57.
23 L. M. M. Quijano and D. A. Singleton, *J. Am. Chem. Soc.*, 2011, **133**, 13824.
24 J. Rehbein and B. K. Carpenter, *Phys. Chem. Chem. Phys.*, 2011, **13**, 20906.
25 J. M. Bowman and B. C. Shepler, *Annu. Rev. Phys. Chem.*, 2011, **62**, 531.
26 B. K. Carpenter, *Chem. Rev.*, 2013, **113**, 7265.
27 M. Paranjothy, R. Sun, Y. Zhuang and W. L. Hase, *J. Comput. Mol. Sci.*, 2013, **3**, 296.
28 T. C. Correra and J. M. Riveros, *J. Phys. Chem. A*, 2010, **114**, 11910.
29 M. A. F. de Souza, T. C. Correra, J. M. Riveros and R. L. Longo, *J. Am. Chem. Soc.*, 2012, **134**, 19004.
30 A. Ricci, *Int. J. Mass Spectrom. and Ion Proc.*, 1997, **164**, 121.
31 Experimental ΔH° values were derived from the values of neutrals and ions tabulated by J. Bartmess, in *Negative Ion Energetics Data*, ed. P. J. Linstrom and W. G. Mallard, NIST Chemistry WebBook, NIST Standard Reference Database Number 69, National Institute of Standards and Technology, Gaithersburg MD, US, 2013, pp. 20899.
32 A. P. Bento, M. Solà and F. M. Bickelhaupt, *J. Chem. Theory Comput.*, 2008, **4**, 929.
33 M. Swart, M. Solá and F. M. Bickelhaupt, *J. Chem. Theory Comput.*, 2010, **6**, 3145.
34 Y. Zhao and D. G. Truhlar, *J. Chem. Theory Comput.*, 2010, **6**, 1104.
35 M. J. Frisch, G. W. Trucks, H. B. Schlegel, G. E. Scuseria, M. A. Robb, J. R. Cheeseman, G. Scalmani, V. Barone, B. Mennucci, G. A. Petersson, H. Nakatsuji, M. Caricato, X. Li, H. P. Hratchian, A. F. Izmaylov, J. Bloino, G. Zheng, J. L. Sonnenberg, M. Hada, M. Ehara, K. Toyota, R. Fukuda, J. Hasegawa, M. Ishida, T. Nakajima, Y. Honda, O. Kitao, H. Nakai, T. Vreven, J. A. Montgomery Jr., J. E. Peralta, F. Ogliaro, M. Bearpark, J. J. Heyd, E. Brothers, K. N. Kudin, V. N. Staroverov, R. Kobayashi, J. Normand, K. Raghavachari, A. Rendell, J. C. Burant, S. S. Iyengar, J. Tomasi, M. Cossi, N. Rega, J. M. Millam, M. Klene, J. E. Knox, J. B. Cross, V. Bakken, C. Adamo, J. Jaramillo, R. Gomperts, R. E. Stratmann, O. Yazyev, A. J. Austin, R. Cammi, C. Pomelli, J. W. Ochterski, R. L. Martin, K. Morokuma, V. G. Zakrzewski, G. A. Voth, P. Salvador, J. J. Dannenberg, S. Dapprich, A. D. Daniels, Ö. Farkas, J. B. Foresman, J. V. Ortiz, J. Cioslowski and D. J. Fox, Gaussian 09 (Revision A.2), Gaussian Inc., Wallingford CT, 2009.
36 M. S. Gordon and M. W. Schmidt, in *Theory and Applications of Computational Chemistry*: *the first forty years*, ed. C. E. Dykstra, G. Frenking, K. S. Kim and G. E. Scuseria, Elsevier, Amsterdam, 2005, pp. 1167.
37 M. W. Schmidt, K. K. Baldridge, J. A. Boatz, S. T. Elbert, M. S. Gordon, J. H. Jensen, S. Koseki, N. Matsunaga, K. A. Nguyen, J. S. Su, T. L. Windus, M. Dupuis and J. A. Montgomery, *J. Comput. Chem.*, 1993, **14**, 1347.
38 V. Lotrich, N. Flocke, M. Ponton, A. D. Yau, P. A., E. Deumens and R. J. Bartlett, *J. Chem. Phys.*, 2008, **128**, 194104.
39 C. M. Aikens, S. P. Webb, R. L. Bell, G. D. Fletcher, M. W. Schmidt and M. S. Gordon, *Theor. Chem. Acc.*, 2003, **110**, 233.
40 C. M. Moller and M. S. Plesset, *Phys. Rev.*, 1934, **46**, 618.
41 C. J. Cramer, in *Essentials of Computational Chemistry*: *Theories and Models*, John Wiley & Sons, Ltd., New York, 2004.
42 K. Raghavachari and G. W. Trucks, *Chem. Phys. Lett.*, 1989, **157**, 479.
43 R. A. Kendall, T. H. Dunning and R. J. Harrison, *J. Chem. Phys.*, 1992, **96**, 6796.
44 D. E. Woon and T. H. Dunning, *J. Chem. Phys.*, 1994, **100**, 2975.
45 A. Halkier, T. Helgaker, P. Jorgensen, W. Klopper, H. Koch, J. Olsen and A. K. Wilson, *Chem. Phys. Lett.*, 1998, **286**, 243.
46 D. G. Truhlar, *Chem. Phys. Lett.*, 1998, **294**, 45.
47 S. B. Huh and J. S. Lee, *J. Chem. Phys.*, 2003, **118**, 3035.
48 A. D. Becke, *J. Chem. Phys.*, 1993, **98**, 5648.
49 C. Adamo and V. Barone, *J. Chem. Phys.*, 1999, **110**, 6158.
50 B. J. Lynch, P. L. Fast, M. Harris and D. G. Truhlar, *J. Phys. Chem. A*, 2000, **104**, 4811.
51 T. Yanai, D. P. Tew and N. C. Handy, *Chem. Phys. Lett.*, 2004, **393**, 51.
52 W. T. Keal and J. D. Tozer, *J. Chem. Phys.*, 2005, **123**, 121103.
53 Y. Zhao, N. E. Schultz and D. G. Truhlar, *J. Chem. Theory Comput.*, 2006, **2**, 364.
54 S. Grimme, *J. Chem. Phys.*, 2006, **124**, 034108.
55 Y. Zhao and D. G. Truhlar, *Theor. Chem. Acc.*, 2008, **120**, 215.
56 J. D. Chai and M. H. Gordon, *J. Chem. Phys.*, 2008, **128**, 084106.
57 J. D. Chai and M. H. Gordon, *Phys. Chem. Chem. Phys.*, 2008, **10**, 6615.
58 A. Karton, A. Tarnopolsky, J. F. Lamère, G. S. Schatz and J. M. L. Martin, *J. Phys. Chem. A*, 2008, **112**, 12868.
59 T. Baer and W. L. Hase, in *Unimolecular Reaction Dynamics. Theory and Experiments*, Oxford, New York, 1996.
60 T. Beyer and D. F. Swinehart, *Commun. ACM*, 1973, **16**, 379.
61 N. A. Pradie and H. V. Linnert, SuperRRKM, version 1.0, University of São Paulo, São Paulo, Brazil. The SuperRRKM is based on: L.

Zhu and W. L. Hase, in *A General RRKM Program*, Department of Chemistry, Wayne State University, 2009, pp. 1993.
62 R. J. Pliego Jr. and J. M. Riveros, *Chem. Eur. J.*, 2001, **7**, 169.
63 D. K. Papayannis, E. Drougas and A. M. Kosmas, *Chem. Phys.*, 2002, **282**, 305.
64 R. J. Pliego Jr. and J. M. Riveros, *J. Phys. Chem. A*, 2002, **106**, 371.
65 C. Adlhart and E. Uggerud, *Phys. Chem. Chem. Phys.*, 2006, **8**, 1066.
66 Y. H-G and J. S. Francisco, *J. Phys. Chem. A*, 2009, **113**, 12932.
67 G. W. Snedecor and W. G. Cochran, in *Statistical Methods*, Iowa State University Press., Ames, 1989.
68 W. L. Hase, *Science*, 1994, **266**, 998.
69 M. L. Chabinyc, S. L. Craig, C. K. Regan and J. I. Brauman, *Science*, 1998, **279**, 1882.
70 J. M. Farrar, *Annu. Rev. Phys. Chem.*, 1995, **46**, 525.
71 S. Moran, H. B. Ellis Jr., D. J. DeFrees, A. D. McLean and G. B. Ellison, *J. Am. Chem. Soc.*, 1987, **109**, 5996.
72 C. Acosta-Silva and V. Branchadell, *J. Phys. Chem. A*, 2007, **111**, 12019.
73 S. Cagnina, P. Rotureau, G. Fayet and C. Adamo, *Phys. Chem. Chem. Phys.*, 2013, **15**, 10849.
74 M. Korth and S. Grimme, *J. Chem. Theory Comput.,*2009, **5**, 993.
75 H. C. Fang, Z. H. Li and K. N. Fan,*Phys. Chem. Chem. Phys.*, 2011, **13**, 13358.

